University of Wollongong
Research Online

Australian Institute for Innovative Materials - Papers

Australian Institute for Innovative Materials

2015

Detection of a Superconducting Phase in a Two-Atom Layer of Hexagonal Ga Film Grown on Semiconducting GaN(0001)

Hui-Min Zhang
Chinese Academy of Sciences

Yi Sun
Peking University, sunyi@ict.ac.cn

Wei Li
Tsinghua University

Jun-Ping Peng
Chinese Academy of Sciences

Canli Song
Tsinghua University

See next page for additional authors

Detection of a Superconducting Phase in a Two-Atom Layer of Hexagonal Ga Film Grown on Semiconducting GaN(0001)

Abstract

The recent observation of the superconducting state at atomic scale has motivated the pursuit of exotic condensed phases in two-dimensional (2D) systems. Here we report on a superconducting phase in twomonolayer crystalline Ga films epitaxially grown on wide-band-gap semiconductor GaN(0001). This phase exhibits a hexagonal structure and only 0.552 nm in thickness, nevertheless, brings about a superconducting transition temperature Tc as high as 5.4 K, confirmed by in situ scanning tunneling spectroscopy and ex situ electrical magnetotransport and magnetization measurements. The anisotropy of critical magnetic field and Berezinski-Kosterlitz-Thouless-like transition are observed, typical for the 2D superconductivity. Our results demonstrate a novel platform for exploring atomic-scale 2D superconductors, with great potential for understanding the interface superconductivity

Keywords

layer, two-atom, phase, detection, semiconducting, grown, gan(0001), film, superconducting, ga, hexagonal

Disciplines

Engineering | Physical Sciences and Mathematics

Authors

Hui-Min Zhang, Yi Sun, Wei Li, Jun-Ping Peng, Canli Song, Ying Xing, Qinghua Zhang, Jia-Qi Guan, Zhi Li, Yanfei Zhao, Shuaihua Ji, Lili Wang, Ke He, Xi Chen, Lin Gu, Langsheng Ling, Mingliang Tian, Lian Li, X. C Xie, Jianping Liu, Hui Yang, Qi-Kun Xue, Jian Wang, and Xu-Cun Ma

Detection of a Superconducting Phase in a Two-Atom Layer of Hexagonal Ga Film Grown on Semiconducting GaN(0001)

Hui-Min Zhang,[1] Yi Sun,[2] Wei Li,[3] Jun-Ping Peng,[1] Can-Li Song,[3] Ying Xing,[2] Qinghua Zhang,[1] Jiaqi Guan,[1] Zhi Li,[1] Yanfei Zhao,[2] Shuaihua Ji,[3,4] Lili Wang,[3,4] Ke He,[3,4] Xi Chen,[3,4] Lin Gu,[1,4] Langsheng Ling,[5] Mingliang Tian,[5] Lian Li,[6] X. C. Xie,[2,4] Jianping Liu,[7] Hui Yang,[7] Qi-Kun Xue,[3,4] Jian Wang,[2,4,*] and Xucun Ma[1,3,4,†]

[1]*Institute of Physics, Chinese Academy of Sciences, Beijing 100190, China*
[2]*International Center for Quantum Materials, School of Physics, Peking University, Beijing 100871, China*
[3]*State Key Laboratory of Low-Dimensional Quantum Physics, Department of Physics, Tsinghua University, Beijing 100084, China*
[4]*Collaborative Innovation Center of Quantum Matter, 100084 Beijing, China*
[5]*High Magnetic Field Laboratory, Chinese Academy of Sciences, Hefei 230031, Anhui, China*
[6]*Department of Physics, University of Wisconsin, Milwaukee, Wisconsin 53211, USA*
[7]*Suzhou Institute of Nano-Tech and Nano-Bionics, Chinese Academy of Sciences, Jiangsu 215123, China*
(Received 4 October 2014; revised manuscript received 26 November 2014; published 10 March 2015)

The recent observation of the superconducting state at atomic scale has motivated the pursuit of exotic condensed phases in two-dimensional (2D) systems. Here we report on a superconducting phase in two-monolayer crystalline Ga films epitaxially grown on wide-band-gap semiconductor GaN(0001). This phase exhibits a hexagonal structure and only 0.552 nm in thickness, nevertheless, brings about a superconducting transition temperature T_c as high as 5.4 K, confirmed by *in situ* scanning tunneling spectroscopy and *ex situ* electrical magnetotransport and magnetization measurements. The anisotropy of critical magnetic field and Berezinski-Kosterlitz-Thouless-like transition are observed, typical for the 2D superconductivity. Our results demonstrate a novel platform for exploring atomic-scale 2D superconductors, with great potential for understanding the interface superconductivity.

Superconductivity has recently been observed in one-atomic-layer Pb and In films grown on a Si(111) substrate [1–7], at the $SrTiO_3/LaAlO_3$ interface [8], and in one-unit-cell thick FeSe films on $SrTiO_3$ [9,10]. This has been stimulating great attention and interest for both understanding the electron pairing in quantum confined systems and also the pursuit of emergent phases of matter in the two-dimensional (2D) systems, such as the enhancement of the superconducting transition temperature T_c. The recent discovery of electric field induced superconductivity at the $SrTiO_3$ surface [11] and in 2D MoS_2 crystal [12] further demonstrates the feasibility of controlling 2D superconductivity via interface engineering. Thus far, however, the nature of interface or 2D superconductivity remains elusive. Preparing more hybrid heterostructures with enhanced superconductivity is necessary but experimentally challenging.

GaN, a wide-band-gap semiconductor with a high piezoelectric constant [13,14], is commonly used in high-speed transistors, lasers for telecommunications, and light-emitting diodes for energy efficient displays. More significantly, it has been previously shown that GaN is often wetted with 1 to 2 atomic layers of Ga atoms [15–17], wherein Ga is intrinsically superconductive [18–20]. Therefore, Ga/GaN may possibly serve as an ideal system to search for enhanced superconductivity near their interface. In this work, by *in situ* scanning tunneling

microscopy and spectroscopy (STM and STS), *ex situ* electrical magnetotransport and magnetization measurements, we have unambiguously demonstrated that two-monolayer (ML) Ga films (as thin as 0.552 nm) grown on GaN form a hexagonal structure and exhibit superconductivity with a T_c up to 5.4 K, which differs from any previously reported stable or crystalline Ga phases [18–20]. The anisotropy of critical magnetic field and Berezinski-Kosterlitz-Thouless (BKT)-like transition are observed, indicative of the 2D nature of superconductivity in 2 ML Ga/GaN(0001).

Our STM and STS experiments are conducted in a Unisoku ultrahigh vacuum low temperature STM system interconnected to a molecular beam epitaxy (MBE) chamber for film preparation. The base pressure is lower than 2×10^{-10} Torr. All Ga films are epitaxially grown on 3 μm thick GaN(0001), which are deposited by metal organic chemical vapor deposition onto $Al_2O_3(0001)$ substrates with a 25 nm AlN buffer layer. The substrates are cleaned by ethanol and acetone before being transferred into the MBE chamber. After degassing at 300 °C for 3 h, several cycles of argon ion sputtering (700 V, 2×10^{-6} Torr) and subsequent annealing in Ga flux are performed to remove contaminations on the surface. Two monolayers of Ga are then epitaxially grown at 650 °C from a high-purity Ga (99.995%) source with a nominal beam flux of 0.4 ML/min. A polycrystalline Pt-Ir tip is used for all

STM and STS investigations. All differential conductance dI/dV spectra are acquired using a standard lock-in technique with a bias modulation of 0.2 mV at 987.5 Hz. For *ex situ* transmission electron microscopy (TEM) and transport measurements, insulating GaN substrates are used, and ~80 nm-thick granular (~10 nm in size) Ag, acting as a protective and capping layer, is deposited on Ga films at 110 K before exposing the sample to the atmosphere. Note that insulating amorphous Si capping layer has also been tried. However, we find that the Si significantly deteriorates the 2 ML Ga thin films on GaN and strongly suppresses their superconductivity.

Figure 1(a) shows the morphology of an atomically flat Ga film. The terraces, which are on average 150 nm wide, are separated by 2.5 Å height steps, consistent with a Ga-N bilayer unit cell along the [0001] direction. Figure 1(b) depicts the atomically resolved STM and its corresponding FFT image, which exhibits a hexagonal lattice with a lattice constant of 3.18 Å, close to that of the underlying GaN(0001) substrate (3.19 Å). Since any previously reported stable and metastable Ga phases show either an orthorhombic or monoclinic symmetry [Table S1] [21,22], the observed 2 ML Ga films with hexagonal lattice are most likely stabilized by the wurtzite structure of the underlying GaN(0001) substrate, and linked to the pseudo 1×1 phase
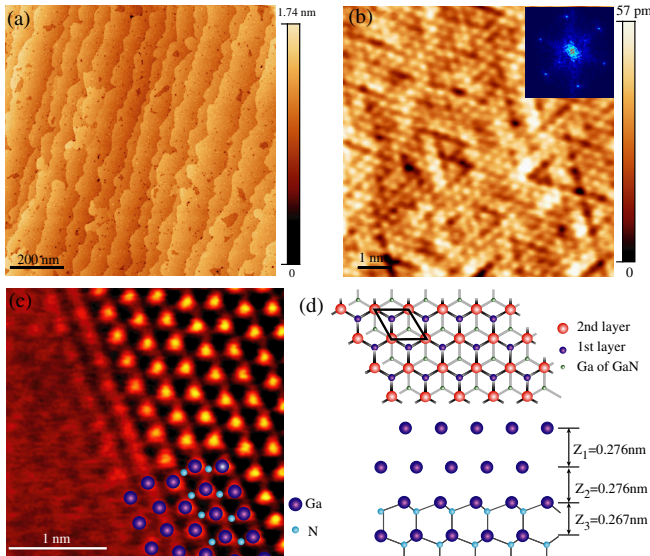
at room temperature [16,17]. The TEM experiment reveals a sharp Ga/GaN(0001) interface and a Ga coverage of 2 ML, directly adjacent to the GaN substrate [Fig. 1(c)]. The spacing between the two Ga layers and GaN substrate is estimated to be 0.276 nm, as schematically sketched in Fig. 1(d).

By taking differential conductance dI/dV spectra on 2 ML Ga films at various temperatures ranging from 2.4 to 6 K [Fig. 2(a)], we observe a series of temperature-dependent superconducting gaps with two clear coherence peaks at ±1.6 meV. The measured gaps reconcile well with the well-known BCS s-wave Dynes function with a broadening factor Γ [23], as illustrated in Fig. S1 [22]. The best fits of the data to BCS gap function [24] yield $\Delta(0) = 1.01 \pm 0.05$ meV, $T_c \sim 5.2$ K, and BCS ratio $2\Delta/k_B T_c = 4.5 \pm 0.2$ (k_B is the Boltzmann constant) [Fig. 2(b)], indicative of a strong coupling superconductor for 2 ML Ga/GaN(0001) [18]. Figure 2(c) illustrates the dI/dV spectra as a function of the applied magnetic field normal to the sample surface ($B_\perp$). With increasing $B_\perp$, the zero bias conductance progressively increases and both the superconducting coherence peaks gradually smear out, providing solid evidence of superconductivity in 2 ML Ga films. It is worth noting that here T_c exceeds 5 K, 5 times higher than 1.08 K for bulk stable α-Ga phase [18].

The high T_c in 2 ML Ga/GaN(0001) has been further corroborated by our systematic transport measurements. Figure 3(a) displays the sample sheet resistance (R_{sheet}) as a

FIG. 1 (color online). (a) Topographic image (3.0 V, 0.05 nA, $1 \times 1 \ \mu m^2$) of 2 ML Ga films, with a step height of 2.5 Å. (b) Atomic-resolution STM image (0.22 V, 0.05 nA, $8 \times 8 \ nm^2$) of a Ga film, and the inset is its corresponding FFT pattern. The bright spots correspond to Ga atoms at the top layer. (c) Cross-sectional high-angle annular dark-field image of Ag/Ga/GaN(0001) heterostructure viewed from the $[11\bar{2}0]$ crystallographic direction, showing two Ga atomic layers just above the GaN substrate. (d) Schematic top (top panel) and section (bottom panel) views of 2 ML Ga/GaN heterostructure. The average separations between various layers are $Z_1 = 2.76$, $Z_2 = 2.76$, and $Z_3 = 2.67$ Å.
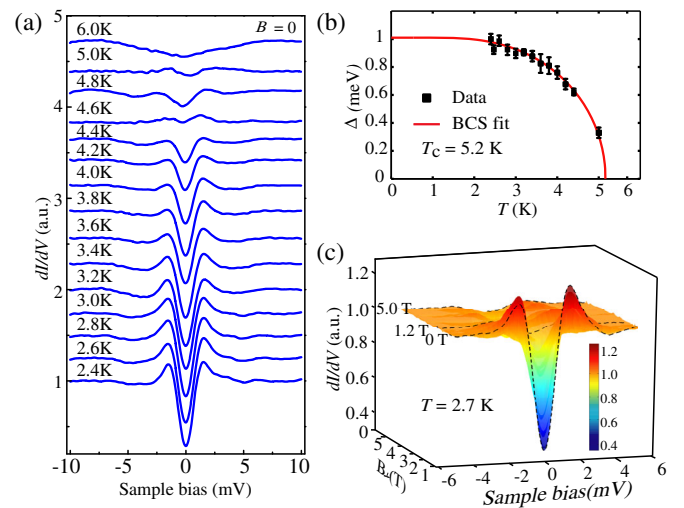

FIG. 2 (color online). (a) A series of differential tunneling conductance spectra (set point: 10 mV, 0.1 nA) at various temperatures, normalized to the normal conductance spectrum at 10 K. (b) Temperature-dependent superconducting gap magnitude Δ (dark squares) and their best fit to BCS gap function (red curve) for 2 ML Ga films. (c) Three-dimensional plots of tunneling conductance measured at various magnetic fields at 2.7 K. Spectra measured at 0, 1.2, and 5.0 T are labeled by black dashes.
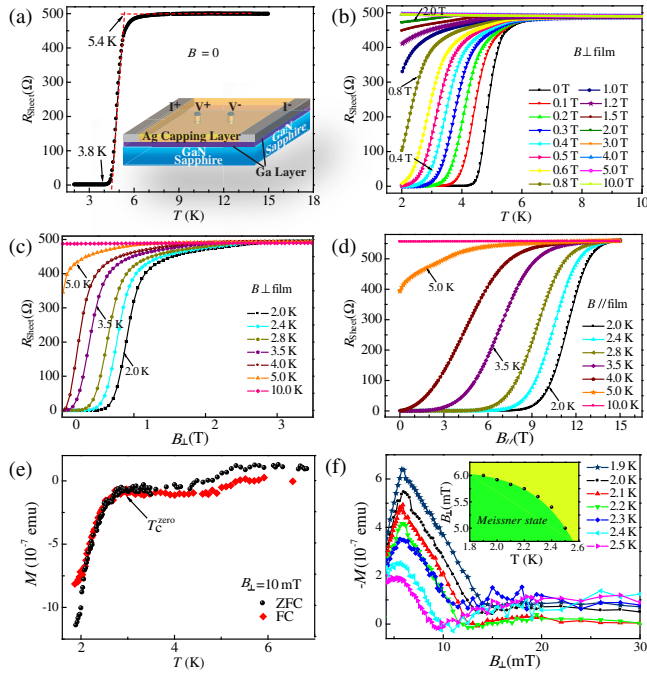
FIG. 3 (color online). (a) R_{sheet}-T curve at zero magnetic field, showing $T_c^{\text{onset}} = 5.4$ and $T_c^{\text{zero}} = 3.8$ K, respectively. The inset schematically shows the diagram for all transport measurements, where indium has been used for all electrical contacts. (b) R_{sheet}-T curves for various $B_\perp$ up to 10 T. (c),(d) Magnetoresistance (c) R_{sheet}-$B_\perp$ and (d) R_{sheet}-$B_\parallel$ at various temperatures ranging from 2.0 to 10 K. (e) Temperature dependence of magnetization measured under a 10 mT magnetic field normal to the sample surface, showing the Meissner effect. (f) Low-field $M(B_\perp)$ at various temperatures from 1.9 to 2.5 K. Note that the magnetization signal below ~4 mT is too small to be resolved in our measurement. Inset shows the temperature dependence of $B_{c1}(T)$. The excitation current of 5 μA is used for all R_{sheet}-T and R_{sheet}-B measurements throughout this Letter.
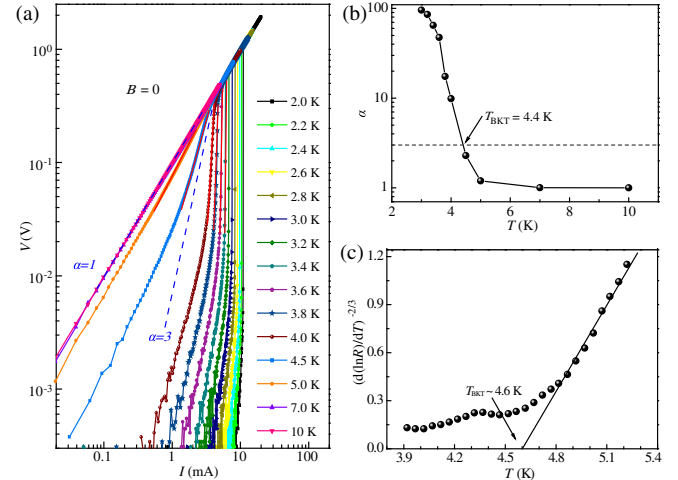

FIG. 4 (color online). (a) $V(I)$ characteristics at various temperatures plotted on a double-logarithmic scale at $B = 0$ T. Two dashed blue lines indicate the $V \sim I$ and $V \sim I^3$ curves, respectively. (b) Plot of the exponent α as a function of temperature T, extracted from the power-law fits in (a). $T_{\text{BKT}} = 4.4$ K is defined as the temperature with $\alpha = 3$. (c) $[d\ln(R_{\text{sheet}})/dT]^{-2/3}$ plotted as a function of temperature. The solid line depicts the expected BKT-like transition behavior with $T_{\text{BKT}} = 4.6$ K.

function of temperature at zero field, with the logarithmic-scale R_{sheet}-T curve shown in Fig. S2 [22]. The superconductivity transition is immediately evident, with $T_c^{\text{onset}} = 5.4$ K, consistent with our STS measurements above. Below 3.8 K, the sample shows zero resistance within our instrumental resolution (± 15 nV). Figure 3(b) shows the R_{sheet} as a function of temperature at different $B_\perp$. The superconductivity transition gets broader and shifts to lower temperature as the field $B_\perp$ increases, as expected. In addition, magnetotransport measurements are carried out at various temperatures between 2.0 and 10.0 K, with the fields normal [Fig. 3(c)] and parallel [Fig. 3(d)] to the sample surface, respectively. It is clearly evident that R_{sheet} varies differently with $B_\perp$ and $B_\parallel$. For example, $R_{\text{sheet}}(B_\perp)$ reaches the normal resistance at ~3.26 T (the upper critical field B_{c2}), substantially smaller than $B_c = 14.8$ T (the critical field) for the parallel field at 2 K. Nevertheless, both critical fields appear significantly greater than $B_c = 5.83$ mT for bulk α-Ga [25], which

may originate primarily from the reduced dimensionality of 2 ML Ga. The small discrepancy of normal-state resistance in Figs. 3(c) and 3(d) may be due to degradation-related aging effect of the sample, because we conducted the out-of-plane field measurements first. The anisotropy in observed critical fields provides the first direct evidence of a typical 2D superconductor behavior for 2 ML Ga/GaN(0001). This is further confirmed by analyzing the temperature dependence of the characteristic magnetic fields $B_\perp(T)$ and $B_\parallel(T)$ [26]. Here $B_\perp(T) \propto 1 - T/T_c$ and $B_\parallel(T) \propto (1 - T/T_c)^{1/2}$ are found, highly suggestive of 2D superconductivity [27] with an estimated superconducting layer thickness of ~5.5 nm [Fig. S3]. Moreover, diamagnetic measurements in Fig. 3(e) shows the dc magnetization as a function of temperature during the zero-field cooling (ZFC) and field cooling (FC) at a perpendicular magnetic field of $B_\perp = 10$ mT. An apparent drop appears slightly below 3.0 K, indicating the Meissner effect. The $M(B_\perp)$ curves at various temperatures are shown in Fig. 3(f), all of which exhibit the expected linear behavior at low fields (≤ 5 mT). At around B_{c1} (the lower critical field), they deviate from linearity, with temperature-dependent B_{c1} plotted in the inset of Fig. 3(f). All these observations provide compelling evidence for the superconductivity in 2 ML Ga/GaN(0001).

To shed further light into the nature of the superconductivity in 2 ML Ga/GaN(0001), Figure 4(a) shows $V(I)$ characteristics at various temperatures ranging from 2 to 10 K. A $V \sim I^\alpha$ power-law dependence is apparently

observed (red lines), with the slope equal to the exponent α. It is found that α reduces with increasing temperature [Fig. 4(b)], consistent with a BKT-like transition [8]. The exponent α approaches 3 at ~4.4 K, identified as T_{BKT}. Furthermore, close to T_{BKT} the measured R_{sheet} depends on temperature via $R_{\text{sheet}}(T) = R_0 \exp[-b(T/T_{\text{BKT}} - 1)^{-1/2}]$, where R_0 and b are material-dependent parameters [8]. This is well illustrated in Fig. 4(c), yielding $T_{\text{BKT}} = 4.6$ K, which matches with the α exponent analysis above. Note that the transition observed here is not sharp as theoretically expected, quite similar to previous experimental reports in the LaAlO$_3$/SrTiO$_3$ interface superconducting system [8] and other quasi-2D superconducting systems, such as FeSe films on SrTiO$_3$ [10] and Pb films on Si(111) [28]. The broad transition might result from the finite size effect or interface effect, which has been demonstrated to play an important role in the non-freestanding quasi-2D superconducting systems [1–10].

We now comment on the role of the Ag capping layer for *ex situ* transport and magnetization measurements. One may wonder whether the metallic Ag will suppress the superconductivity of 2 ML Ga films due to proximity effect [29–32]. Indeed, as demonstrated in Fig. 5, the proximity induced superconductivity in the Ag layer (blue dashes) accompanied with the suppressed superconductivity in Ga films are clearly identified by comparing dI/dV spectra before (black curve) and after (black and blue dashes) Ag deposition. Previous study has revealed that the T_c of a superconductor or normal metal bilayer system decays exponentially with the thickness ratio of normal metal and superconductor [29]. In our case, 2 ML Ga films are only 0.552 nm thick, while the Ag capping layer is 80 nm thick. Thus, if the Ag layer is in good contact with Ga films, it would mean an almost complete suppression of superconductivity in a Ag/Ga bilayer. The robust superconductivity observed here therefore appears quite unexpected and surprising. Two possible explanations might be considered. First, the ultrathin Ga films are not freestanding, but supported by a GaN substrate, which may help preserve the superconductivity. Second, the capping Ag layer exists in the form of nanoparticles with a typical size of ~10 nm, comparable to $\xi_{ab}\sim$ 10 nm deduced from $B_{c2} \sim 3.26$ T by $B_{c2} = \Phi_0/2\pi\xi_{ab}^2$. Therefore, not all Ga film surface is in direct contact with Ag. Instead there may be spaces between the Ag nanoparticles and the underlying Ga films. As a consequence, the proximity effect develops only in a small minority of regions with Ag contacting the underlying 2 ML Ga films, leaving most other regions unaffected. These regions may percolate throughout the whole films and form an infinite superconducting percolating network, which leads to the superconducting behaviors detected by transport measurements and BKT-like transition [33]. Further theoretical and
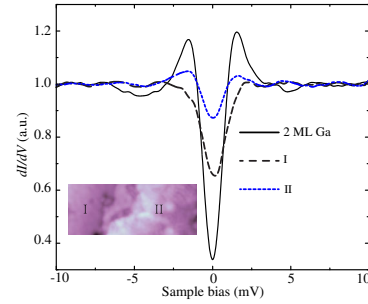

FIG. 5 (color online). Normalized dI/dV spectra before and after Ag deposition. Inset shows 2 ML Ga (I) partially covered by 1 ML Ag (II) (1.8 V, 0.05 nA, 25×10 nm^2). Three spectra are acquired at pristine Ga films (solid black curve), regions I (black dashes) and II (blue dashes), respectively.

experimental investigations in this context would be helpful to fully resolve this issue.

Finally, we remark on the possible mechanism of high T_c in 2 ML Ga/GaN(0001) hybrid heterostructure. One may expect that the dimensionality effect plays a role. However, previous studies have shown strongly suppressed superconductivity as a superconductor gets thinner [34,35]. It is therefore unlikely that the observed high T_c of 5.4 K stems solely from the dimensionality effect. In analogy to recent studies [4,9,10], we suggest that the superconductivity observed here may originate from the interface effect between Ga and GaN. The closely matched lattice constants suggest the possible strong interface interactions between Ga and GaN. On the other hand, GaN has a noncentrosymmetric crystal structure and may exhibit a strong polarization effect [13], which can enhance superconductivity at the Ga/GaN interface. In fact, the 2D electron gas, a prerequisite for superconductivity, is indeed observed in wurtzite heterostructures such as AlGaN/GaN [14], which has been explained as polarization effect induced interface charge accumulation.

In summary, 2 ML Ga films with hexagonal atomic structure have been successfully grown on a GaN(0001) substrate and demonstrated to be 2D superconductors by both *in situ* STM and STS and *ex situ* electrical magneto-transport and magnetization measurements. Compared to the stable α-Ga phase, T_c in 2 ML Ga/GaN(0001) is considerably enhanced. Our finding may provide a 2D system for uncovering the nature of interface superconductivity. All STM images were processed by Nanotec WSxM software [36].

*jianwangphysics@pku.edu.cn
†xucunma@mail.tsinghua.edu.cn

[1] Y. Guo, Y.-F. Zhang, X.-Y. Bao, T.-Z. Han, Z. Tang, L.-X. Zhang, W.-G. Zhu, E. G. Wang, Q. Niu, Z. Q. Qiu, J.-F. Jia, Z.-X. Zhao, and Q.-K. Xue, Science **306**, 1915 (2004).

[2] M. M. Özer, J. R. Thompson, and H. H. Weitering, Nat. Phys. **2**, 173 (2006).

[3] S. Qin, J. Kim, Q. Niu, and C.-K. Shih, Science **324**, 1314 (2009).

[4] T. Zhang, P. Cheng, W.-J. Li, Y.-J. Sun, G. Wang, X.-G. Zhu, K. He, L. Wang, X. Ma, X. Chen, Y. Wang, Y. Liu, H.-Q. Lin, J.-F. Jia, and Q.-K. Xue, Nat. Phys. **6**, 104 (2010).

[5] C. Brun, T. Cren, V. Cherkez, F. Debontridder, S. Pons, D. Fokin, M. C. Tringides, S. Bozhko, L. B. Ioffe, B. L. Altshuler, and D. Roditchev, Nat. Phys. **10**, 444 (2014).

[6] T. Uchihashi, P. Mishra, M. Aono, and T. Nakayama, Phys. Rev. Lett. **107**, 207001 (2011).

[7] M. Yamada, T. Hirahara, and S. Hasegawa, Phys. Rev. Lett. **110**, 237001 (2013).

[8] N. Reyren, S. Thiel, A. D. Caviglia, L. F. Kourkoutis, G. Hammerl, C. Richter, C. W. Schneider, T. Kopp, A.-S. Rüetschi, D. Jaccard, M. Gabay, D. A. Muller, J.-M. Triscone, and J. Mannhart, Science **317**, 1196 (2007).

[9] Q.-Y. Wang, Z. Li, W.-H. Zhang, Z.-C. Zhang, J.-S. Zhang, W. Li, H. Ding, Y.-B. Ou, P. Deng, K. Chang, J. Wen, C.-L. Song, K. He, J.-F. Jia, S.-H. Ji, Y.-Y. Wang, L.-L. Wang, X. Chen, X.-C. Ma, and Q.-K. Xue, Chin. Phys. Lett. **29**, 037402 (2012).

[10] W.-H. Zhang, Y. Sun, J.-S. Zhang, F.-S. Li, M.-H. Guo, Y.-F. Zhao, H.-M. Zhang, J.-P. Peng, Y. Xing, H.-C. Wang, T. Fujita, A. Hirata, Z. Li, H. Ding, C.-J. Tang, M. Wang, Q.-Y. Wang, K. He, S.-H. Ji, X. Chen, J.-F. Wang, Z.-C. Xia, L. Li, Y.-Y. Wang, J. Wang, L.-L. Wang, M.-W. Chen, Q.-K. Xue, and X.-C. Ma, Chin. Phys. Lett. **31**, 017401 (2014).

[11] K. Ueno, S. Nakamura, H. Shimotani, A. Ohtomo, N. Kimura, T. Nojima, H. Aoki, Y. Iwasa, and M. Kawasaki, Nat. Mater. **7**, 855 (2008).

[12] J. T. Ye, Y. J. Zhang, R. Akashi, M. S. Bahramy, R. Arita, and Y. Iwasa, Science **338**, 1193 (2012).

[13] F. Bernardini, V. Fiorentini, and D. Vanderbilt, Phys. Rev. B **56**, R10024 (1997).

[14] O. Ambacher, J. Smart, J. R. Shealy, N. G. Weimann, K. Chu, M. Murphy, W. J. Schaff, L. F. Eastman, R. Dimitrov, L. Wittmer, M. Stutzmann, W. Rieger, and J. Hilsenbeck, J. Appl. Phys. **85**, 3222 (1999).

[15] Q.-K. Xue, Q. Xue, R. Bakhtizin, Y. Hasegawa, I. S. T. Tsong, T. Sakurai, and T. Ohno, Phys. Rev. Lett. **82**, 3074 (1999).

[16] G. F. Sun, Y. Liu, Y. Qi, J. F. Jia, Q. K. Xue, M. Weinert, and L. Li, Nanotechnology **21**, 435401 (2010).

[17] J. E. Northrup, J. Neugebauer, R. M. Feenstra, and A. R. Smith, Phys. Rev. B **61**, 9932 (2000).

[18] W. Gregory, T. Sheahen, and J. Cochran, Phys. Rev. **150**, 315 (1966).

[19] H. Parr and J. Feder, Phys. Rev. B **7**, 166 (1973).

[20] R. Cohen, B. Abeles, and G. Weisbarth, Phys. Rev. Lett. **18**, 336 (1967).

[21] Z. Liu, Y. Bando, M. Mitome, and J. Zhan, Phys. Rev. Lett. **93**, 095504 (2004).

[22] See Supplemental Material at http://link.aps.org/supplemental/10.1103/PhysRevLett.114.107003 for details on the BCS fit of the dI/dV spectrum, crystallographic data of Ga phases, and transport measurements.

[23] R. C. Dynes, V. Narayanamurti, and J. P. Garno, Phys. Rev. Lett. **41**, 1509 (1978).

[24] J. Bardeen, L. N. Cooper, and J. R. Schrieffer, Phys. Rev. **108**, 1175 (1957).

[25] L. I. Berger and B. W. Roberts, *Properties of Superconductors*, edited by David R. Lide, CRC Handbook of Chemistry and Physics (CRC Press, Boca Raton, 2004).

[26] N. Reyren, S. Gariglio, A. D. Caviglia, D. Jaccard, T. Schneider, and J.-M. Triscone, Appl. Phys. Lett. **94**, 112506 (2009).

[27] M. Tinkham, noop McGraw-Hill, Inc., New York **93**, 94 (1996).

[28] W. Zhao, Q. Wang, M. Liu, W. Zhang, Y. Wang, M. Chen, Y. Guo, K. He, X. Chen, Y. Wang, J. Wang, X. Xie, Q. Niu, L. Wang, X. Ma, J. K. Jain, M. Chan, and Q.-K. Xue, Solid State Commun. **165**, 59 (2013).

[29] L. Cooper, Phys. Rev. Lett. **6**, 689 (1961).

[30] Z. Long, M. D. Stewart, T. Kouh, and J. M. Valles, Phys. Rev. Lett. **93**, 257001 (2004).

[31] I. Sternfeld, V. Shelukhin, A. Tsukernik, M. Karpovski, A. Gerber, and A. Palevski, Phys. Rev. B **71**, 064515 (2005).

[32] S. Bose and P. Ayyub, Phys. Rev. B **76**, 144510 (2007).

[33] G. M. Wysin, A. R. Pereira, I. A. Marques, S. A. Leonel, and P. Z. Coura, Phys. Rev. B **72**, 094418 (2005).

[34] C. Brun, I.-Po Hong, F. Patthey, I. Yu. Sklyadneva, R. Heid, P. M. Echenique, K. P. Bohnen, E. V. Chulkov, and W.-D. Schneider, Phys. Rev. Lett. **102**, 207002 (2009).

[35] C. L. Song, Y. L. Wang, Y. P. Jiang, Z. Li, L. Wang, K. He, X. Chen, X. C. Ma, and Q. K. Xue, Phys. Rev. B **84**, 020503 (2011).

[36] I. Horcas, R. Fernandez, J. M. Gomez-Rodriguez, J. Colchero, J. Gómez-Herrero, and A. M. Baro, Rev. Sci. Instrum. **78**, 013705 (2007).